Ultrasonics Sonochemistry 21 (2014) 1893–1899

Contents lists available at ScienceDirect

Ultrasonics Sonochemistry

journal homepage: www.elsevier.com/locate/ultson

Electrochemical investigations of stable cavitation from bubbles generated during reduction of water

M. Keswani *, S. Raghavan, P. Deymier

Department of Materials Science and Engineering, The University of Arizona, 1235 E James E Rogers Way, Tucson, AZ 85721, USA

ARTICLE INFO

Article history:
Received 1 September 2012
Received in revised form 16 April 2014
Accepted 16 April 2014
Available online 24 April 2014

Keywords:
Megasonic cleaning
Stable cavitation
Microstreaming
Hydrogen bubbles
Water reduction
Chronoamperometry

ABSTRACT

Megasonic cleaning is traditionally used for removal of particles from wafer surfaces in semiconductor industry. With the advancement of technology node, the major challenge associated with megasonic cleaning is to be able to achieve high cleaning efficiency without causing damage to fragile features. In this paper, a method based on electrochemistry has been developed that allows controlled formation and growth of a hydrogen bubbles close to a solid surface immersed in an aqueous solution irradiated with ~1 MHz sound field. It has been shown that significant microstreaming from resonating size bubble can be induced by proper choice of transducer duty cycle. This method has the potential to significantly improve the performance of megasonic cleaning technology through generation of local microstreaming, interfacial and pressure gradient forces in close vicinity of conductive surfaces on wafers without affecting the transient cavitation responsible for feature damage.

1. Introduction

Megasonic cleaning is one of the common techniques used for removal of particles from wafer surfaces in semiconductor industry [1,2]. However, with the advancement of technology node to 22 nm and lower, the feature size is becoming increasingly small and fragile while the requirements for cleaning are becoming more stringent [3]. In order to be able to continue the use of megasonic technology for wafer cleaning, it is essential to identify new cleaning mechanisms that will allow high particle removal without causing damage to fine features.

During megasonic exposure of liquids, two primary phenomena/mechanisms are known to exist, namely, acoustic streaming and cavitation [4–6]. Acoustic streaming is the time independent motion of a fluid due to viscous attenuation and can be classified into four different types: Eckart streaming, Schlichting streaming, Rayleigh streaming, and Microstreaming [7]. In acoustic cavitation, bubbles form and grow in size by rectified diffusion or coalescence driven by either primary or secondary Bjerknes forces [8]. Some bubbles continuously oscillate for many acoustic cycles (stable cavitation) while others collapse (transient cavitation) typically in less than one cycle. Microstreaming, which is a consequence of large oscillations of stable bubbles, can cause significant fluid flow surrounding the bubbles [9]. It is generally believed that microstreaming plays an important role in removal of particles during megasonic cleaning of wafers while feature damage is primarily caused by transient cavitation [9,10]. Development of an effective megasonic cleaning process that can achieve high particle removal efficiency (PRE) with minimum damage is possible through enhancement of microstreaming, interfacial and pressure gradient forces [11] without affecting transient cavitation.

There have been several studies in the past that have focused on understanding the behavior of stable and transient cavities and their associated physical and chemical effects [12–15]. Birkin et al. investigated the growth of a 2 mm radius bubble due to rectified diffusion as well as mass transfer from microstreaming using an acoustoelectrochemical technique employing a 25 μm Pt microelectrode [15]. The bubble radius growth rate was determined to be ~0.03 μm/s in aerated potassium ferricyanide containing aqueous solutions irradiated with a sound field of 2.08 kHz at 51.74 Pa. In another study using a 25 μm Pt microelectrode, Maisonhaute et al. examined single bubble oscillatory behavior in aqueous solutions subjected to 500 kHz sound frequency at power density of 1.4 W/cm^2 [16]. The current transients consisting of 'peaks' with life times of a few milliseconds observed during high time resolution chronoamperometry measurements were attributed to flux of ferricyanide species towards the electrode surface from microstreaming resulting from oscillations of stable bubbles . At lower sound frequency of 20 kHz, bubbles of sizes up to 0.8 mm oscillating at harmonics of driving frequency were observed [17,18]. It was suggested that the shape of the bubbles was hemispherical

* Corresponding author. Tel.: +1 (520)270 4361; fax: +1 (520)621 8059.
E-mail address: manishk@email.arizona.edu (M. Keswani).

http://dx.doi.org/10.1016/j.ultsonch.2014.04.009
1350-4177/

rather than spherical and the bubbles exhibited transient as well as quasi-stable cavitation behavior. Other studies conducted using microelectrodes (6–25 μm) in the ultrasonic frequency range (20–100 kHz) have shown that mass transfer induced by transient cavitation is much higher than that by acoustic streaming [19,20]. Keswani et al. characterized transient cavitation under ~1 MHz sound field using high time resolution cyclic voltammetry and chronoamperometry techniques in aqueous solutions containing additives such as dissolved gases (Ar, N_2 or CO_2) or non-ionic surfactants (Triton X®-100 or NCW®-1002) [21,22]. Their results revealed that dissolved Ar and non-ionic surfactants increase the intensity of transient cavity collapses while dissolved CO_2 significantly reduces it.

As can be noticed from aforementioned studies, most of the work in literature has been directed towards understanding the role of acoustic cavitation and streaming during sonic exposure of liquids. In order to enhance the performance of megasonic processes for wafer cleaning, it is important to not only develop fundamental understanding of current cleaning mechanisms but also devise new methods that will likely improve cleaning. In the current work, electrochemical investigations of microstreaming in aqueous solutions have been carried out using a Pt microelectrode *at potentials where water reduction occurs*. Under these conditions, significant microstreaming from oscillating hydrogen bubbles (depending on the transducer percent duty cycle) was observed as indicated by current 'transients' during chronoamperometry measurements. This technique can benefit the semiconductor industry through its further development for improved megasonic cleaning of conductive surfaces. Although, the micro-electrode based electrochemical set-up used in our experimental investigations offers the major advantage of detecting single bubble activity in a multi-bubble environment, it can't be used for monitoring multiple bubbles at the same time (which requires an array of micro-electrodes).

2. Materials and methods

High purity (99.9%) chemicals (potassium ferricyanide ($K_3Fe(CN)_6$) and potassium chloride (KCl)) were purchased from Sigma Aldrich. Platinum wires (99%) were procured from Goodfellow. The electrode set up, pre-cleaning procedures and placement of electrodes in the megasonic system used for the experiments have been described elsewhere [21]. The electrodes were positioned facing down parallel to the transducer surface. The transducer power density was fixed at 2 W/cm^2 while percent duty cycle was varied between 10% and 100% for 5 ms pulse time [22]. Aqueous solutions containing 0.1 M KCl with and without 50 mM ($K_3Fe(CN)_6$) were prepared using high purity de-ionized (DI) water of resistivity 18 Mohm-cm. Ferricyanide, being an electroactive species, is used as an electrochemical probe in this study to monitor the bubble behavior. The experimental solutions were saturated with Ar gas by bubbling for 30 min and keeping the Ar blanket over the liquid surface during the measurements. The removal of dissolved O_2 was confirmed by measuring the oxygen level using an oxygen sensor (Rosemount 152 Analytical model 499A DO).

Chronoamperometry experiments were conducted using a function generator Agilent 33250A with a custom built potentiostat equipped with positive feedback ohmic drop compensation (constructed by Mike Read, ChIEF, University of Arizona) described in [23]. Measurements were performed with and without application of potential at −2 V (*versus Pt reference or −1.4 V versus standard hydrogen electrode (SHE)*) in the absence and presence of megasonic field at ~1 MHz. The data were acquired at a high sampling rate of 8 MHz using an oscilloscope (NI USB-5133). NI LabVIEW 9.0 and DIAdem™ 2010 were used for data acquisition and graphical processing, respectively.

3. Results and discussion

A first set of experiments was carried out using Ar saturated aqueous solutions containing 0.1 M potassium chloride and no ferricyanide. The results are shown in Fig. 1(a) where the *y*-axis represents current and *x*-axis depicts time. The first 0.5 s of data was collected without any applied potential and megasonic energy. During this time, no current was measured. After 0.5 s, a potential of −2.0 V (*versus* Pt) was applied to the working electrode (25 μm) at which time the current shoots up to a steady or limiting value of 20–25 μA. Since the applied potential is far more negative than the standard reduction potential of water (−0.83 V), the limiting current may be attributed to reduction of water to hydrogen gas and hydroxyl ion. Upon application of megasonic field at 100% duty cycle (DC) after 1 s of applied potential, the limiting current shows 'valleys' superimposed on it.

Fig. 1(b) displays examples of these current 'valleys' with expanded time scale. The fall or dip times of 'valleys' range from 8 μs to 0.3 ms with majority of them occurring between 0.1 and 0.3 ms time scale while the rise was found to vary from 0.1 to 0.3 ms. We interpret the fall in current as possibly due to the formation and growth of hydrogen bubbles in the close vicinity of the electrode surface. Due to continuous generation of hydrogen gas at the electrode surface, there is enough gas available to form and grow oscillating bubbles by rectified diffusion [24]. It is to be noted that the bubble may not be composed of only hydrogen gas but may also partly contain the gas that is dissolved in the liquid as will be evident from the results in the later sections. As the bubbles grow, they mask the electrode surface, which causes the current to fall. After some time, bubbles have grown to sizes that exceed the acoustic boundary layer thickness and are swept away from the electrode surface due to the liquid flow from acoustic streaming and the current recovers to the limiting value. After the megasonic field is switched off at ~3.5 s, the current 'valleys' no longer appear on the limiting current. When the megasonic field is applied at 10% duty cycle, the current–time data, illustrated in Fig. 1(c), shows mostly noise in current and hardly any current 'valleys'. At 10% duty cycle, the screening of the electrode due to hydrogen bubbles may not be efficient enough due to the formation of (a) a smaller number of bubbles close to the electrode surface and (b) not enough time for the bubbles to grow beyond the resonating size (~3.8 μm radius at ~1 MHz sound frequency) by rectified diffusion. In this case, since the area blocked by few small bubbles is much smaller than the electrode area, it does not lead to any measureable drop in current.

Fig. 2(a) through (f) show the effect of addition of potassium ferricyanide on the measured current at different percent duty cycle (for fixed pulse time of 5 ms) for Ar saturated aqueous KCl solution irradiated with megasonic field. In all these cases, the working electrode was biased at −2.0 V (*versus* Pt reference) throughout the experiment. Firstly, the current is measured in the absence of megasonic field for <1.6 s, then the megasonic field is turned on for 2 s followed by last ~0.5–1 s of current measurement again in the absence of megasonic field. The limiting current in the absence of megasonic field was approximately constant at 20–25 μA, as in the previous case with no ferricyanide, indicating that the current due to ferricyanide reduction (measured to be 0.3 μA in [22]) is negligible compared to that due to water reduction.

At 10% duty cycle, corresponding to the transducer on and off times of 0.5 and 4.5 ms, respectively, the results shown in Fig. 2(a) and (b) indicate current 'peaks' riding on the limiting current. These current 'peaks' exhibit a rise time of 0.5 ms (same as the transducer on time) and fall time of <1 ms. The maximum current reached by peaks is ~85 μA with many peaks

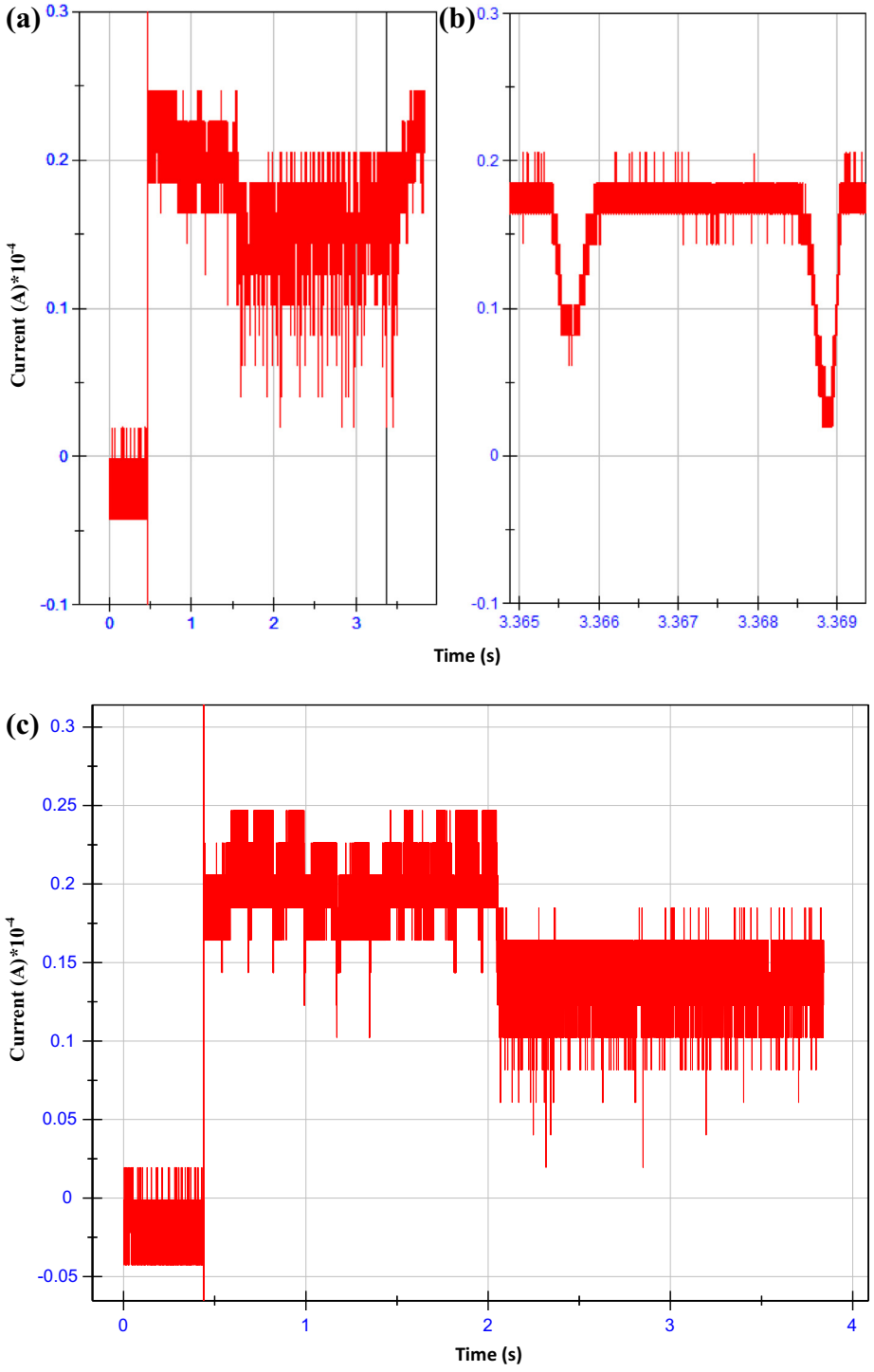

Fig. 1. Chronoamperometry measurements on 25 μm Pt microelectrode in Ar saturated aqueous solutions containing 0.1 M potassium chloride without any potassium ferricyanide: (a) and (b) 100% duty cycle with full time scale and expanded time scale respectively, (c) 10% duty cycle with full time scale.

crossing ~70 μA. Fig. 3(a) shows an example of current 'peak' with expanded time scale. After the initial rise of current (for <0.1 ms) oscillations with large amplitude (~20–30 μA) occur with an oscillating frequency corresponding to that of the megasonic field (~1 MHz). This observation is interpreted as follows: (a) a small number of bubbles are nucleated and start oscillating with the acoustic field when the megasonic field is turned on, (b) bubbles grow to resonant size by diffusion of hydrogen gas from the surrounding liquid due to continuous water reduction and the bubbles' oscillation amplitude increases, (c) bubbles attain a resonant size (~3.8 μm radius at ~1 MHz sound frequency) after about 0.3 ms and exhibit high amplitude oscillations. The increase in current upon application of megasonic field can be attributed to enrichment of ferricyanide by advection [25,21] followed by its subsequent diffusion every time bubble shrinks during its oscillation. However, when the bubble oscillations are large, the current is significantly affected not only by advection based diffusion of ferricyanide but also by transport of ferricyanide towards and away from the electrode surface due to microstreaming (reflected in the form of oscillating current). After the megasonic field is

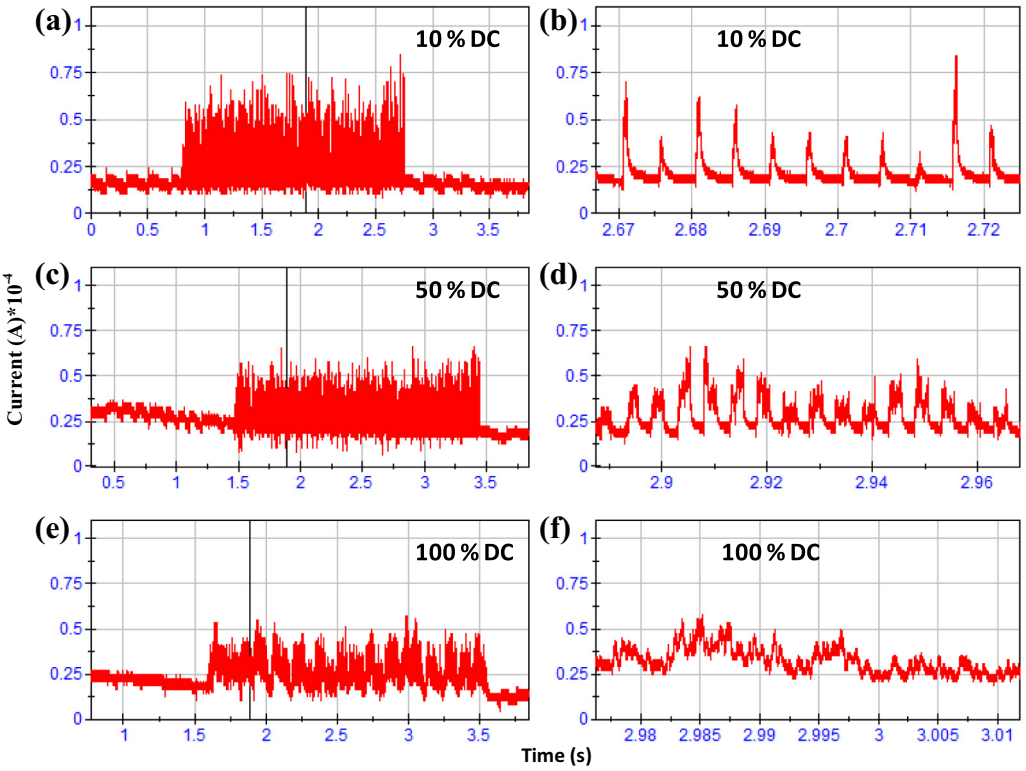

Fig. 2. Effect of transducer duty cycle on chronoamperometry current for experiments conducted using 25 μm Pt microelectrode in Ar saturated aqueous solutions containing 0.1 M potassium chloride and 50 mM potassium ferricyanide.

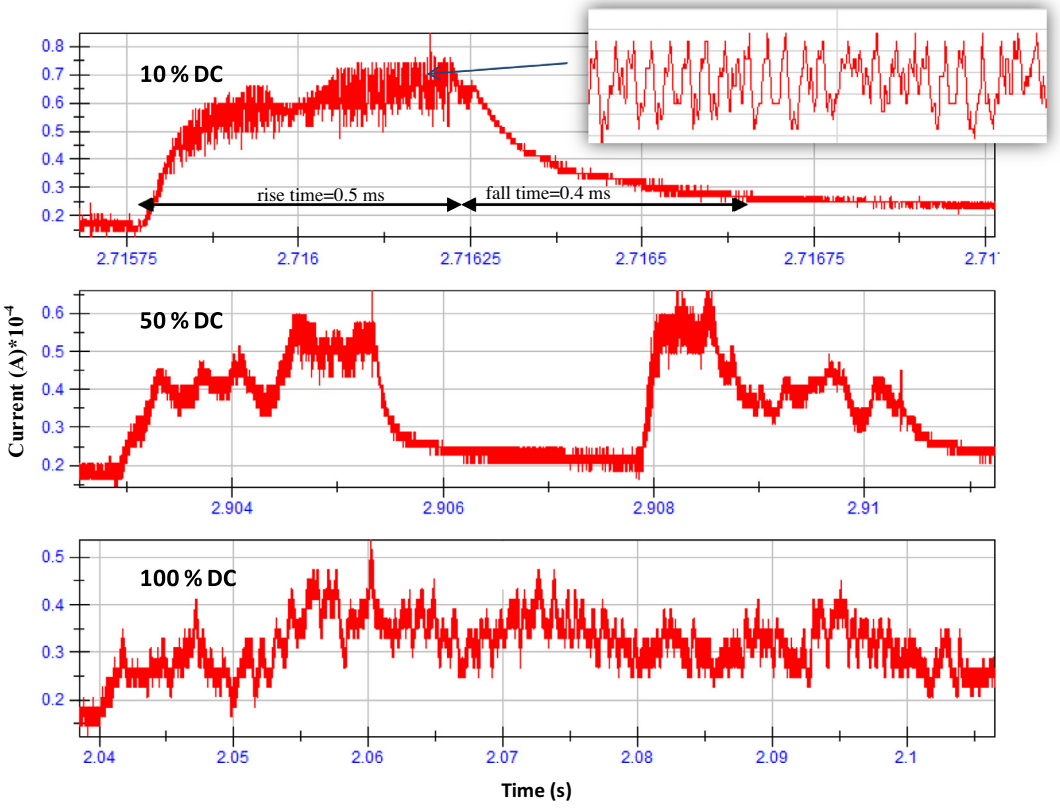

Fig. 3. Data similar as that in Fig. 2 but with expanded time scale to demonstrate current transients.

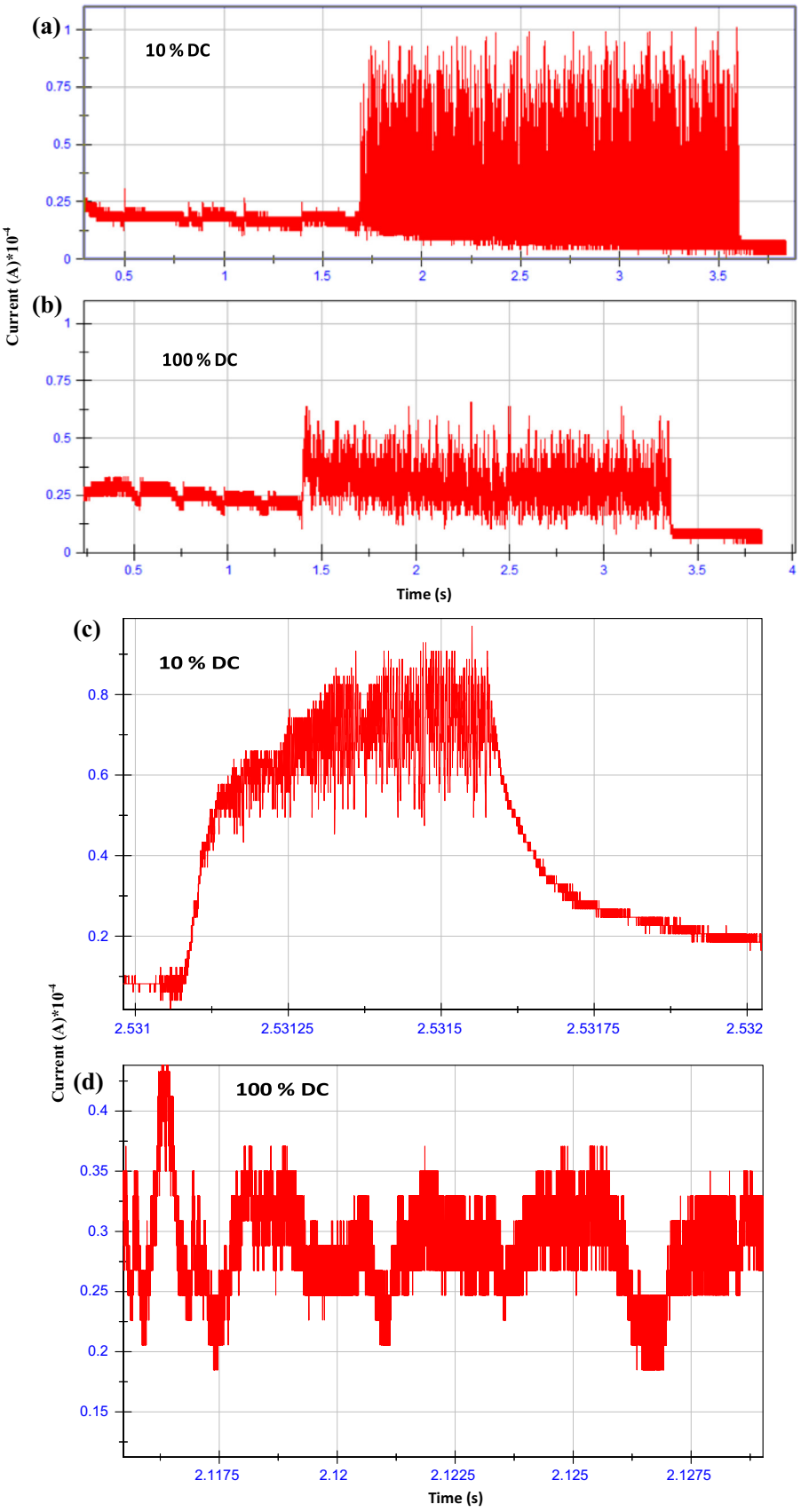

Fig. 4. Effect of transducer duty cycle on chronoamperometry current for experiments conducted using 25 μm Pt microelectrode in CO_2 saturated aqueous solutions containing 0.1 M potassium chloride and 50 mM potassium ferricyanide (a and b) full time scale and (c and d) expanded time scale.

stopped, the current fall back to the limiting value. Using the steady current value of 20 μA, the time taken by a single bubble to reach the resonant size can be approximately computed assuming that diffusion of hydrogen gas into the bubble is fast enough and rate of hydrogen generation is the limiting step. Since two electrons are required to produce one hydrogen molecule during reduction of water ($2H_2O_{(l)}+2e^- \leftrightarrow H_{2(g)} + 2OH^-_{(aq)}$), a current of 20 μA would correspond to 1.25×10^{14} electrons per second or 6.2×10^{13} hydrogen molecules per second [26]. At 25 °C and 1 atm, a bubble of radius 3.8 μm (or volume 2.3×10^{-16} m^3) would have 5.7×10^9 molecules assuming ideal gas behavior. Therefore, the bubble reaches the resonant size in ~0.1 ms, which is on the same order of magnitude but slightly smaller than the rise time of 'peaks' possibly due to the assumption that all hydrogen produced goes into the formation of a single bubble. Once the bubble reaches a resonant size, it is likely to experience the streaming flow, which moves it away from the electrode. The acoustic boundary layer thickness (δ) at 1 MHz sound frequency in DI water is ~0.5 μm calculated using $\delta = (\nu/\omega)^{0.5}$, where ν is the kinematic viscosity of water and ω is the angular acoustic frequency. When the bubble is close to resonant size, a large portion of it is outside the acoustic boundary and therefore experiences the streaming flow. The fall time of bubble can be estimated as follows. The streaming velocities have been reported to be between 0 and 1.5 cm/s for sound frequencies of 0.5–4 MHz [11,27]. Taking the maximum streaming velocity of 1.5 cm/s and assuming that the bubble has to move across the radius of the microelectrode (12.5 μm), the time taken by the bubble to completely pass the electrode would be ~0.8 ms, which is close to that observed in our experiments. A shorter time might indicate that the cavity is lifted off the electrode plane before crossing its resonant radius.

At 50% duty cycle, (see Fig. 2(c) and (d)), a similar behavior is observed where current 'peaks' are superimposed on the limiting current during the application of megasonic field. However, unlike the case of 10% duty cycle, the current does not increase steadily during the transducer "on-time". Instead, the current rises and falls a few times as can be seen from Fig. 3(b), where examples of current 'peaks' are shown with expanded time scale. Furthermore, the maximum current measured for 50% duty cycle was 65 μA, which is lower than that measured for 10% duty cycle. This is most likely because the recovery time or the transducer off-time at 50% duty cycle (~2.5 ms) is not sufficient to allow all the gaseous bubbles present in the solution to dissolve away during the transducer on time. These residual bubbles that survive the transducer off-time interfere with the behavior of new bubbles that form and grow with the beginning of each megasonic cycle. This is further evident from results of 100% duty cycle displayed in Fig. 2(e) and (f) as well as in Fig. 3(c) which shows that the maximum current in this case is the lowest (~55 μA). Additionally, the current appears to vary significantly during the application of megasonic field possibly due to multiple bubbles interacting with each other at the same time. It is essential at this stage to point out an important difference in the results for the two cases of with and without ferricyanide. In the absence of ferricyanide, at 100% duty cycle, even though multiple tiny residual bubbles from previous cycle(s) may be present, the drop in current is unlikely to be affected when the mechanism is primarily blocking of electrode by growing bubbles. Once the electrode is partially blocked, any interference from another bubble (that forms or passes between the growing bubble and the microelectrode) is undetected. However, in the presence of ferricyanide, when the rise in current is due to diffusion, advection and microstreaming, the current values are likely to be affected via interferences between multiple oscillating bubbles.

In order to determine if the reported bubble behavior (in the earlier sections) is predominantly that of a hydrogen bubble, experiments were performed in CO_2 saturated potassium chloride solutions containing potassium ferricyanide. The sequence of applying and removing the megasonic field was the same as that for the previous experiments. The results for 10% and 100% duty cycle are illustrated in Fig. 4(a) through (d) with Fig. 4(c) and (d) showing the expanded time scale. The limiting current measured in the absence of megasonic field was ~20–25 μA. At 10% duty cycle, during megasonic exposure, current 'peaks' with rise time of 0.5 ms and fall time of <1 ms were observed whereas at 100% duty cycle, the current continuously varied with no particular trend. The maximum current measured for 10% duty cycle (~100 μA) was much higher than that measured for 100% duty cycle (~65 μA). These current values are somewhat higher than those measured in the case of Ar saturated solution indicating that the bubble behavior is partially influenced by the gas dissolved in the liquid. This suggests that the bubble may not be purely a hydrogen gas bubble but may also contain some other gas that was dissolved in the liquid as well as any gases (e.g. O_2, Cl_2) that may be liberated at the anode. Additionally, since dissolved CO_2 is known to drastically reduce transient cavitation [28–30], presence of significant current 'peaks' in CO_2 saturated solution (during megasonic irradiation) for experiments conducted in this study, provides further evidence to the fact that the measured current 'peaks' are due to stable oscillating bubbles and not collapsing cavities.

4. Conclusions

In the current work, we have been able to successfully form and grow stable bubbles to a resonating size close to a solid conducting surface by applying a potential of −2 V and controlling the transducer duty cycle. At 10% duty cycle, resonating bubbles exhibited high amplitude oscillations, reflected in the form of oscillating current, which caused significant fluid flow due to microstreaming. At higher percent duty cycles of 50% and 100%, the overall current was lower due to interference between bubbles that survived during the transducer off time. These results can be extremely useful for megasonic cleaning in semiconductor industry where strong microstreaming can be generated close to the conducting surfaces on wafers without being concerned about transient cavitation. Higher streaming flow is likely to enhance particle removal without causing damage to delicate features on patterned wafers.

Acknowledgements

We acknowledge support from NSF Grant ECCS-0925340. We also thanks ProSys Inc. for loaning the megasonic equipment.

References

[1] M. Keswani, S. Raghavan, P. Deymier, S. Verhaverbeke, Microelectron. Eng. 86 (2) (2009) 132–139.
[2] W. Kern, Handbook of Semiconductor Wafer Cleaning Technology: Science, Technology and Applications, Noyes Publications, New Jersey, 1993.
[3] ITRS, The International Technology Roadmap for Semiconductors, http://www.itrs.net/Links/2011ITRS/Home2011.htm (2011).
[4] P. Deymier, J. Vosseur, A. Khelif, B. Djafari-Rouhani, L. Dobrzynski, S. Raghavan, J. Appl. Phys. 88 (11) (2000) 6821–6835.
[5] F. Young, Cavitation, McGraw-Hill, New York, 1989.
[6] T. Leighton, The Acoustic Bubble, vol. 10, Academic Press, London, 1997.
[7] F. Zhang, A. Busnaina, M. Fury, S. Wang, J. Elelctron. Mater. 29 (2) (2000) 199–204.
[8] K. Yasui, Fundamentals of acoustic cavitation and sonochemistry Chapter 1, in: Pankaj, M. Ashokkumar (Eds.), Theoretical and Experimental Sonochemistry Involving Inorganic Systems, Springer, Netherlands, 2011, pp. 7–8.
[9] G. Gale, A. Busnaina, Part. Sci. Technol. 17 (3) (1999) 229–238.
[10] V. Kapila, P.A. Deymier, H. Shende, V. Pandit, S. Raghavan, F.O. Eschbach, Proc. SPIE-Int. Soc. Opt. Eng. 6283 (2006) 628324/1–628324/12.
[11] W. Kim, T. Kim, J. Choi, H. Kim, Appl. Phys. Lett. 94 (081908) (2009) 1–3.
[12] Y.E. Watson, P.R. Birkin, T.G. Leighton, Ultrason. Sonochem. 10 (2003) 65–69.
[13] P.R. Birkin, Y.E. Watson, T.G. Leighton, K.L. Smith, Langmuir 18 (2002) 2135–2140.

[14] P.R. Birkin, Y.E. Watson, T.G. Leighton, J. Chem. Soc., Chem. Commun. 24 (2001) 2650–2651.
[15] P.R. Birkin, T.G. Leighton, Y.E. Watson, Ultrason. Sonochem. 11 (2004) 217–221.
[16] E. Maisonhaute, F. Javier Del Campo, R. Compton, Ultrason. Sonochem. 9 (463) (2002) 275–283.
[17] E. Maisonhaute, B.A. Brookes, R.G. Compton, J. Phys. Chem. 106 (2002) 3166–3172.
[18] E. Maisonhaute, P.C. White, R.G. Compton, J. Phys. Chem. 105 (2001) 12087–12091.
[19] P. Birkin, C. Delaplace, C. Bowen, J. Phys. Chem. 102 (52) (1998) 10885–10893.
[20] P. Birkin, S. Silva-Martinez, Electroanal. Chem. 416 (1996) 127–138.
[21] M. Keswani, S. Raghavan, P. Deymier, Microelectron. Eng. 102 (2013) 91–97.
[22] M. Keswani, S. Raghavan, P. Deymier, Ultrason. Sonochem. 20 (2013) 603–609.
[23] C. Amatore, C. Lefrou, F. Pflüger, J. Electroanal. Chem. 270 (1989) 43–59.
[24] D. Hsieh, M. Plesset, J. Acoustic Soc. Am. 33 (2) (1961) 206–215.
[25] S. Mishra, P. Deymier, K. Muralidharan, G. Frantziskonis, S. Pannala, S. Simunovic, Ultrason. Sonochem. 17 (2010) 258–265.
[26] A. Yueng, Geochemical processes affecting electrochemical remediation Chapter 3, in: K. Reddy, C. Cameselle (Eds.), Electrochemical Remediation Technologies for Polluted Soils Sediments and Groundwater, Wiley Publication, New york, 2009, p. 732. first ed..
[27] S. Sakamoto, Y. Watanabe, Jpn. J. Appl. Phys. 38 (5B) (1999) 3050–3052.
[28] S. Kumari, M. Keswani, S. Singh, M. Beck, E. Liebscher, P. Deymier, S. Raghavan, Microelectron. Eng. 88 (2011) 3437–3441.
[29] S. Kumari, M. Keswani, S. Singh, M. Beck, E. Liebscher, L.Q. Toan, S. Raghavan, ECS Trans. 41 (2011) 93–99.
[30] M. Keswani, S. Raghavan, R. Govindarajan, I. Brown, Microelectron. Eng. 118 (2014) 61–65.